Noninvasive Auto-Photoreduction Used as a Tool for Studying Structural Changes in Heme-Copper Oxidases by FTIR Spectroscopy

Karin Bettinger, Alexander Prutsch, Karsten Vogtt, and Mathias Lübben
Lehrstuhl für Biophysik, Ruhr-Universität Bochum, D-44780 Bochum, Germany

ABSTRACT We demonstrate an efficient Fourier transform infrared (FTIR) spectroscopic method, termed "auto-photoreduction," that uses anaerobic photo-induced internal electron transfer to monitor reaction-initiated changes of heme-copper oxidases. It can be applied without the use of either expensive electrochemical equipment, or caged compounds, which cause significant background signals. At high irradiation power, carbon monoxide is released from high-spin heme *a* of cytochrome *c* oxidase and heme *o* from cytochrome bo_3. Photochemistry is initiated at wavelengths <355 nm, and the photochemical action spectrum has a maximum of 290 nm for cytochrome bo_3, which is consistent with the possible intermediate involvement of tyrosinate or an activated state of tyrosine. We propose that the final electron donors are proton channel water molecules. In the pH range of 4–9, the noninvasive auto-photoreduction method yields highly reproducible FTIR redox difference spectra within a broad range, resolving a number of vibrational changes outside the amide I region (1600–1640 cm^{-1}). Furthermore, it provides details of redox-induced changes in the spectral region between 1600 and 1100 cm^{-1}. The auto-photoreduction method should be universally applicable to heme proteins.

INTRODUCTION

Cytochrome oxidases are the terminal enzymes of aerobic electron transport phosphorylation (Wikström et al., 1981; Babcock and Wikström, 1992; Ferguson-Miller and Babcock, 1996). They belong to a class of heterooligomeric integral membrane proteins, which form a superfamily of cytochrome *c* or ubiquinol oxidizers (Saraste, 1990; Saraste et al., 1991; Trumpower and Gennis, 1994; Garcia-Horsman et al., 1994; Pereira et al., 2001). The substrate O_2 is bound to the binuclear center of heme a_3 (*o*) and Cu_B; electron transfer to molecular oxygen is coupled to proton uptake for water formation and to proton pumping. Structural analysis of mitochondrial and bacterial oxidases (Iwata et al., 1995; Tsukihara et al., 1996) predicts the existence of two different internal proton transport pathways, the K- and the D-channels, each of which consists of two chains of conserved polar amino acids. The mechanism of proton movement within both pathways, especially across the D-channel, is of particular interest and has been recently studied by various infrared spectroscopic methods (Lübben and Gerwert, 1996; Hellwig et al., 1996, 1998; Lübben et al., 1999; Yamazaki et al., 1999b; Rich and Breton, 2001; Iwaki et al., 2002; Nyquist et al., 2003). Earlier, we assigned redox-induced infrared absorption signals in the carbonyl region of cytochrome bo_3 to an environmental change of the conserved Glu-286 (Lübben et al., 1999). (The numbering of amino acids located in subunit I is based on the sequence of cytochrome bo_3.)

Previously applied techniques to study redox-dependent protonation changes suffer from specific limitations, although the recently reported development of the perfusion technique, using attenuated total reflectance (Nyquist et al., 2001; Rich and Breton, 2002) appears to be promising. However, the spectro-electrochemical cell requires highly concentrated protein solutions and the addition of redox mediators to secure redox equilibration. Moreover, it requires rather demanding technical equipment. On the other hand, the ''caged electron'' approach, using FMN as a photoreductant (termed ''photoreduction''), allowed the use of highly concentrated samples, which were applied as thin hydrated films (Lübben and Gerwert, 1996). Nevertheless, the difference signals in the spectral fingerprint region are significantly superimposed due to high background absorptions from the caged compound itself. (We use the term ''fingerprint region'' operationally to define the region of 1100–1680 cm^{-1}, which provides spectral information on amino acid side chains of proteins.) Slight variations in the photochemical reaction result in great changes and make spectral interpretation in this region a rather complex task. This is because it is intrinsically impossible to subtract the fractional contributions of the caged electron reaction itself from the total absorbance change of the photoreaction, as the light-driven electron transport from the mediator takes place only when a corresponding electron acceptor is present.

Consequently, it is necessary to find a reduction technique that provides reliable insights into the spectral region of 1100–1650 cm^{-1}. As reported earlier, heme proteins, in which the central iron is in the ferric state, can be photoreduced in the absence of external electron donors by irradiation with UV or visible light. Examples for this

Submitted March 8, 2003, and accepted for publication December 15, 2003.

K.B. and A.P. contributed equally to this work.

Address reprint requests to Mathias Lübben, Tel.: +49-234-32-24465; Fax: +49-234-32-14626; E-mail: luebben@bph.rub.de.

Abbreviations used: FTIR, Fourier transform infrared; EDTA, ethylendiamine tetra-acetate; FMN, flavine mononucleotide; HPLC, high-performance liquid chromatography; IR, infrared; MIR, mean infrared (1000–2000 cm^{-1}); Ni-NTA, nickel nitrilo-triacetic acid; UV, ultraviolet.

0006-3495/04/05/3230/11 $2.00

phenomenon are the one-electron transitions found in met-myoglobin, met-hemoglobin or p-450 hydroxylase and cytochrome *c* (Pierre et al., 1982; Bazin et al., 1982; Gu et al., 1993; Sakai et al., 2000). Aerobic light-induced electron transfer has also been examined for mitochondrial cytochrome *c* oxidase (Salmeen et al., 1978; Adar and Yonetani, 1978; Adar and Erecinska, 1979; Babcock and Salmeen, 1979; Ogura et al., 1985; Brooks et al., 1997).

In this report we use anaerobic auto-photoreduction via internal electron transfer to investigate cytochrome oxidases by means of FTIR spectroscopy, namely the ubiquinol oxidase cytochrome bo_3 of *Escherichia coli*, and the cytochrome *c* oxidases of mitochondria and of the proteobacterium *Rhodobacter sphaeroides*. This photochemical autoreduction technique allows the detailed study of the IR fingerprint region, which is known to contain information on absorbances of specific functional groups of proteins.

EXPERIMENTAL PROCEDURES

Preparations of oxidases

Cytochrome bo_3 was isolated from *E. coli* strain BL21 Δ*cyo* (Kan^R), grown in Luria Broth medium in the presence of 50 μg/ml Kanamycin and 50 μg of Ampicillin to select for the cytochrome bo_3 overproducer plasmid pHCL. The oligohistidine-tagged protein was isolated by a previously described procedure (Prutsch et al., 2000) with the following modification: the treatment of membranes with 5 M urea was omitted due to high losses at that stage. The protein was concentrated to 50 mg/ml with Microsep centrifugation cups (Pall-Filtron, Northborough, MA), using 20 mM Tris-Cl, 50 mM NaCl, 0.3% (w/v) β-decylmaltoside, pH 8.0 as a standard (''storage'') buffer. In the pH range 7.0–9.0, aliquots of the pooled fractions from the Ni-NTA column were diluted in the standard buffer, which was adjusted with 0.1 M HCl or 0.1 M NaOH before concentration. For pH 6.0, 20 mM citrate was used instead. Site-directed mutants were constructed and prepared as described above (Lübben et al., 1999; Prutsch et al., 2000).

R. sphaeroides strain YZ100, kindly donated by S. Ferguson-Miller (East Lansing, MI), was grown as described (Zhen et al., 1998). The protocol was modified at the following stages: i), β-*n*-dodecyl maltoside was used as the sole detergent; ii), membrane homogenization was carried out in 10 mM Tris-Cl, 40 mM KCl, pH 8.0; iii), the oxidase was solubilized in wash buffer (150 mM KCl, 20 mM Tris-Cl, 0.3% β-*n*-dodecylmaltoside, pH 7.5) at a membrane protein concentration of 8 mg/ml with 1% detergent; iv), the Ni-NTA column was eluted with 50 mM histidine in wash buffer instead of imidazol; v), the cytochrome *c* oxidase was stored in 10 mM potassium phosphate buffer, 1 mM EDTA, 0.3% β-*n*-dodecylmaltoside, pH 7.5.

Professor Peter Rich (London, UK) kindly donated the mitochondrial cytochrome *c* oxidase.

Other analytical methods

Protein concentration was determined by the bicinchoninic acid method (Smith et al., 1985), with serum albumin as standard. Sodium dodecyl sulfate gel electrophoresis was carried out by the Laemmli method (Laemmli, 1970). Oxidases were quantified with an Aminco (Silver Spring, MD) DW-2 split beam spectrometer using the extinction coefficients (reduced-oxidized enzymes) of 24,000 $M^{-1} \times cm^{-1}$ (605–630 nm) (Vanneste, 1966) for cytochrome *c* oxidase and of 18,700 $M^{-1} \times cm^{-1}$ (560–580 nm) for ubiquinol oxidase (Kita et al., 1984). Heme extraction and HPLC analysis were carried out as described above (Lübben and Morand, 1994). For correction of variable heme recovery, internal standards were added to the samples before extraction; heme B was added to cytochrome *c* oxidase and heme A was added to ubiquinol oxidase samples. Ubiquinol oxidase activity (Prutsch et al., 2000) and cytochrome *c* oxidase activity (Zhen et al., 1998) were tested as previously reported.

Anaerobic semidry sample preparation

Samples were prepared for optical and for FTIR spectroscopy by applying them onto CaF_2 windows and subsequently drying them in vacuo. Aliquots of the oxidases (1–5 μl) containing a total amount of up to 75 μg protein were pipetted into the center of a CaF_2 plate, transferred to a workshop-modified desiccator and dried by membrane pump evacuation for defined time periods (1–5 min). After rehydration with H_2O or D_2O solvents, a CaF_2 counter plate was pressed on top of the first one by means of a glass piston (details of the apparatus used for anaerobic sample preparation will be published elsewhere). This procedure enabled the adjustment of a sample layer thickness to <5 μm. The plate sandwich was sealed with Apiezon grease and placed in a workshop-made cuvette holder.

Anaerobic preparation of liquid samples

For the measurement of oxidase activity after irradiation, the protein samples were diluted (final concentration 0.2 mg/ml) in vacuum-degassed storage buffer. The sample was added to a stoppered quartz cuvette (0.1 mm pathlength) and exposed for 15 min to an argon atmosphere for removal of residual oxygen.

Optical spectroscopy of auto-photoreduced samples

To monitor cytochrome reduction in the photoreduction and auto-photoreduction experiments, optical spectra were recorded with a diode-array spectrophotometer, operated with monitoring light from a halogen lamp in the range of 380–1000 nm. To obtain reasonable signal/noise ratios in the static spectra, 100 scans from an integration period of 0.1 s were averaged. For dynamic measurement of the CO recombination, samples were activated by a flash bulb (20 μs pulse length) and spectra were recorded in logarithmic time intervals over a total observation period of 0.5 s.

Photoirradiation methods

Laser irradiation

The samples were irradiated at 308 nm by a LPX 240i UV excimer laser (Lambda-Physik, Göttingen, Germany) with a pulse energy of 90–100 mJ. Subsequently, the samples were placed in the diode-spectrophotometer after each series of flashes.

Lamp irradiation

When photoreduction was carried out with a Xe arc lamp (150 W; Oriel, Stratford, CT), the light source was adjusted to a 35° angle relative to the monitoring beam at a distance of 50 cm from the sample. The photolytic light intensity was greatly enhanced by placing a focusing quartz lens at the central point of the distance between lamp and sample (25 cm each), and this setting was termed ''high intensity'' conditions. To prevent sample denaturation, the light was heat filtered through an 8-cm cuvette containing water. Photoreduction rates of cytochrome bo_3 were calculated after normalization of spectra to the absorbance value at the isosbestic wavelength of 545 nm (Kita et al., 1984). The degree of reduction was determined from the absorbance difference between 560 and 545 nm of the α-band. For absolute quantification, fully reduced oxidase was prepared by photoreduc-

tion with FMN. The photon fluxes of the Xe lamp intensities in the range of 300–400 nm (UG 1 filter DIN 58191 from Schott Glaswerke, Mainz, Germany) were determined with the chemical actinometer Aberchrome 540 (Heller and Langan, 1981).

Recording of the photochemical action spectrum

To correct the wavelength-dependent emission of the Xe lamp, the monochromatic photon fluxes were quantified from actinometric measurements as described above. To achieve the same arbitrarily selected intensity of 5×10^{18} photons per cm^2 at all wavelengths, the different irradiation times were adjusted accordingly. During sample irradiation, visible spectra were recorded; the absorbance changes at 560 nm indicated the levels of reduction of cytochrome bo_3, which were plotted against the irradiation wavelengths.

FTIR spectroscopy

For routine spectra, 37 μg (samples in H_2O) or 50 μg (samples in D_2O) of cytochrome bo_3 were applied between CaF_2 windows as described above. The exact sample amounts were determined by visible redox difference spectra. About 75 μg of bacterial (*R. sphaeroides*) and mitochondrial cytochrome *c* oxidase was used. Static FTIR spectra were recorded with a Bruker IFS66v instrument (Karlsruhe, Germany), using a 2600 cm^{-1} cutoff filter during all experiments, except for overview spectra taken to assess the degree of solvent isotope exchange. Nominal resolution was set to 2 cm^{-1}; all other conditions were as described above (Lübben et al., 1999). The samples were thermostated at 4°C. Measurements were taken after irradiation periods of 20 s by a Xe lamp (see above) or a 100-W halogen lamp. Four-hundred scans in the single-sided forward/backward acquisition mode with a 100-kHz sampling rate were recorded. These measuring cycles were repeated until no further spectral changes were observed. To correct for possible temporal drifts in absorbance difference spectra, driftline subtraction was allowed using linear functions, extrapolated from absorbance values at three different wave numbers chosen from different regions of the MIR spectra (2000, 1960, and 1250 cm^{-1}). In spectra of cytochrome bo_3, the samples yielded absorbance differences at 1696–1691 cm^{-1} of 0.75×10^{-3}. If minor deviations occurred, these values were used as a reference for scaling the spectra.

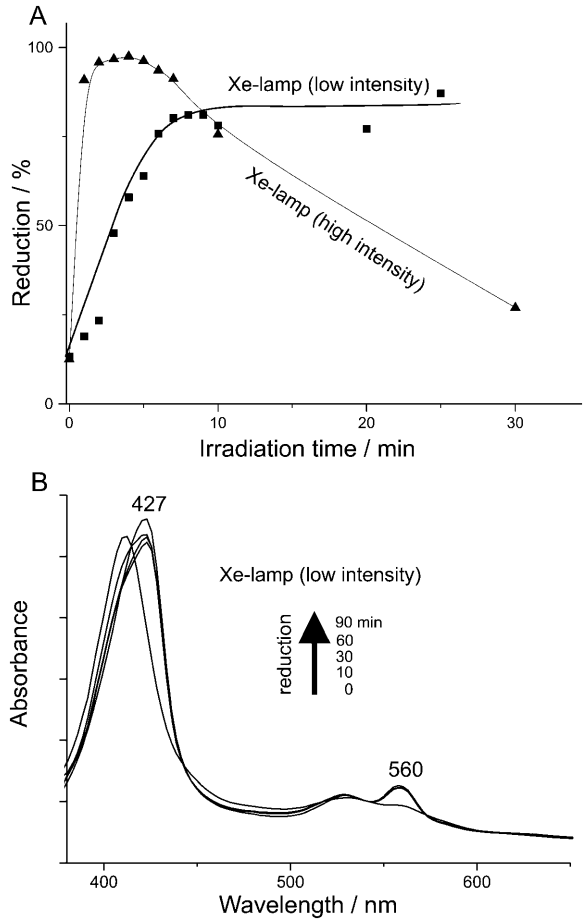

FIGURE 1 (*A*) Auto-photoreduction of cytochrome bo_3 measured with optical spectroscopy. The reduction rates were measured by the heme absorbance changes at 560 nm upon irradiation with light from different sources. High intensity: 150-W Xe lamp, lens focused to a diameter of ~5 mm. Low intensity: 150-W Xe lamp, nonfocused. (*B*) Absorption spectra reflecting the gradual reduction of cytochrome bo_3 after the indicated times of low-intensity irradiation with a Xe lamp.

RESULTS

Optical measurement of auto-photoreduction

When cytochrome bo_3 in thin films without external addition of reductants was exposed anaerobically to light from different sources, we observed relatively high photoreduction rates (Fig. 1 *A*, *triangles*). After ~1000 laser flashes at 308 nm (not shown) or 5 min continual UV irradiation with a Xe lamp at high light intensity (photon flux: 4.4×10^{15} photons per second per cm^2), the oxidase reached almost 100% reduction, whereas prolonged irradiation led to a decrease in absorbance. This is probably due to the damaging effect of high light intensity, which is also accompanied by the photochemical formation of carbon monoxide (see below). Lower light intensity (photon flux: 1.1×10^{15} photons/s/cm^2) required longer irradiation times (Fig. 1, *A* (*squares*) and *B*). Light from a halogen lamp (having a rather low UV content) yielded a very slight degree of reduction within the chosen observation time (not shown). The photoreduction effect of cytochrome bo_3 and of cytochrome *c* oxidase has been tested in the presence of 3, 6, and 10 mM tryptophan as a potential external source of electrons, but the aromatic amino acid known to enhance reduction rates with other heme proteins (Pierre et al., 1982; Bazin et al., 1982; Gu et al., 1993; Sakai et al., 2000) was ineffective when used with cytochrome oxidases.

Exposing a sample to high light intensities, such as those emitted by the UV laser or the focused Xe lamp, rapidly results in the release of carbon monoxide, which then diffuses and concomitantly binds to intact high-spin hemes. This degree of chemical disintegration of the photoreduced cytochrome bo_3 was monitored using time-resolved CO difference spectroscopy. The typical (CO/reduced-*minus*-reduced) difference spectrum (obtained by flash dissociation of the complex; see legend of Fig. 2 for further details) demonstrates that carbon monoxide has been formed during the

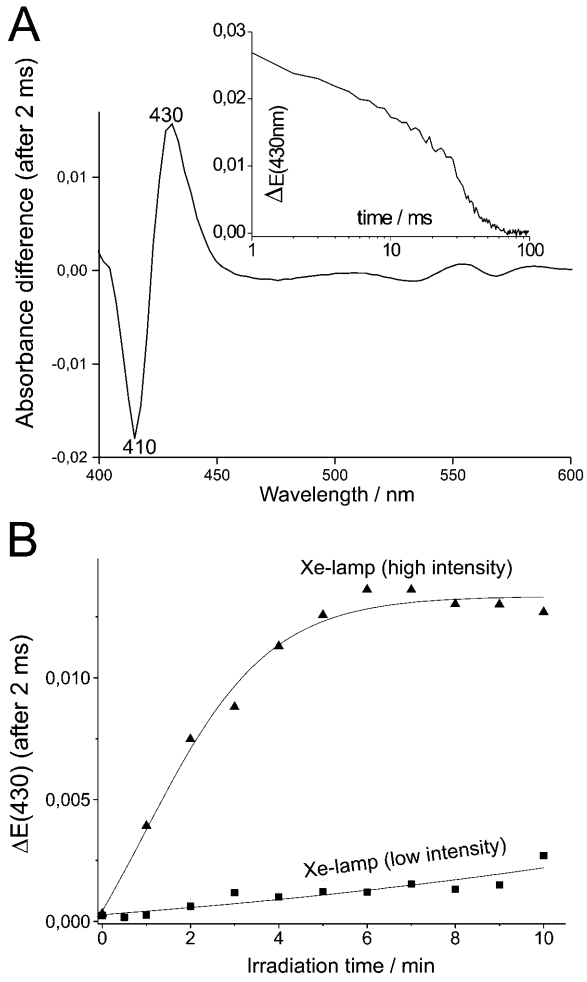

FIGURE 2 (*A*) Demonstration of carbon monoxide formation induced by the auto-photoreduction reaction at high-light intensity. First, cytochrome bo_3 was auto-photoreduced by irradiation with 1000 flashes from excimer laser at 308 nm. To analyze the apparent CO-bound enzyme, the sample was transferred to the diode array spectrometer setup and flash photolysis was initiated with a 20-μs flash bulb pulse. Photochemical difference spectra of the carbon monoxide complex of cytochrome bo_3 (CO bound/reduced-*minus*-reduced) were measured with a diode array spectrometer at a time resolution of 1 ms; only the first spectrum after 2 ms is shown. (*Insert*) The time course of CO recombination, observed by the absorbance difference at 430 nm. (*B*) CO formation under different irradiation conditions. The difference amplitudes at 430 nm (measured 2 ms after flash photolytic activation) were determined after certain intervals of Xe-lamp irradiation at high (*triangles*) or low (*squares*) intensities.

auto-photoreduction reaction. CO was obviously released from certain functional groups located within the protein, as no other potential external sources were present. The identity of carbon monoxide as the ligand, which binds to the binuclear center, is further supported by the characteristic recombination kinetics observed after flash photolysis of the high-spin heme complex (*insert* of Fig. 2 *A*). Carbon monoxide release was negligible when halogen light (not shown) or light from the unfocused Xe lamp was applied (Fig. 2 *B*, *squares*). In contrast, there was a significant release of carbon monoxide during irradiation with the focused Xe lamp (Fig. 2 *B*, *triangles*). Formation of carbon monoxide from cytochrome bo_3 therefore appears to correlate with the intensity of incident UV light.

The process of auto-photoreduction of cytochrome bo_3 is strongly pH dependent. It has a maximum pH of ~7.5 (not shown). The data precision does not allow the determination of exact pK values, but it indicates that at least one protonatable group is involved during a certain stage of the photochemical reaction pathway.

Heme composition of photoreduced oxidases

It has been reported that in met-hemoglobin the protein-associated heme group itself is responsible for internal electron transfer (Sakai et al., 2000). Moreover, it is known that isolated heme B undergoes light-induced reduction in the presence of electron donors (Bartocci et al., 1980). Cytochrome bo_3 carries two heme groups with different chemical structures (Puustinen and Wikström, 1991; Puustinen et al., 1992; Rumbley et al., 1997), namely hemes *b* (hexa-coordinated, low-spin) and *o* (penta-coordinated ligand binding, high-spin). To determine the role of these, the heme composition was analyzed after treatment with light at different intensities. The HPLC traces of the extracted hemes are displayed in Fig. 3. Hemes B and O of the untreated control sample were verified with standard compounds (Prutsch et al., 2000). They exhibited peaks with the expected retention times of 35.6 and 55.3 min. After normalization with respect to their unequal extinction coefficients, the peak areas correspond to a 1:1 ratio of heme B:O (Rumbley et al., 1997). Samples fully reduced by low intensities of the Xe lamp had the same heme composition as the nontreated reference. Upon irradiation with the focused Xe lamp, heme B was shown to be present in similar amounts, but the heme O peak vanished almost completely. The results are summarized in the inset of Fig. 3. The low-spin heme *b* of cytochrome bo_3 remains unchanged, whereas the high-spin ligand binding heme *o* appears to be decomposed by very intense UV light. It is proposed that carbon monoxide is formed by the photodecay of heme *o*. Similar experiments with cytochrome aa_3 of *R. sphaeroides* (not shown) demonstrate heme *a* degradation of >50% under the same conditions. The data suggest that farnesylated hemes are more susceptible to photochemical decomposition combined with CO release. These data do not allow the exclusion of the low-spin heme *a* as a possible target in cytochrome aa_3.

Biochemical activity and protein-chemical stability of auto-photoreduced oxidases

Although conditions of nondisruptive auto-photoreduction at low intensity could be adjusted via estimation of CO release, the enzymatic activity of the oxidases had to be assured. The

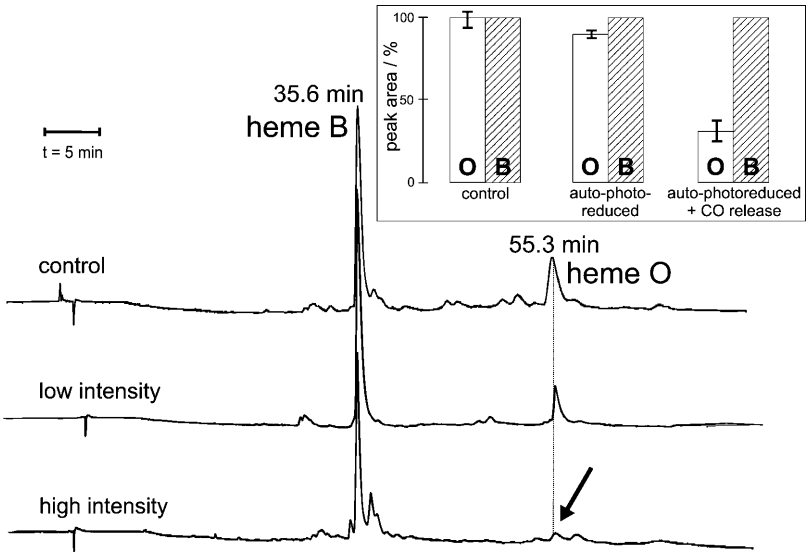

FIGURE 3 Heme analysis of cytochrome bo_3 after photoirradiation. HPLC elution profile of hemes extracted from cytochrome bo_3 from dark control, and of hemes extracted after 60 min photoirradiation with Xe lamp at low-light and intense-light conditions. (*Inset*) Summary of heme analysis, scaled to the (unchanged) heme B content.

reversibility of auto-photoreduction was monitored by optical spectroscopy. Cytochrome bo_3 photoreduced under moderate conditions could be converted back to the oxidized form by adding ferricyanide (data not shown). Almost complete reduction of cytochrome *c* oxidases and ubiquinol oxidase was obtained with insignificant CO release; notably this treatment preserved full enzyme activities (Table 1). However, both cytochromes bo_3 and aa_3 were catalytically inactive after irradiation under CO release conditions. Similarly, inactivation took place when the UV laser was used as a light source. SDS gel electrophoresis was used to verify the protein-chemical integrity of cytochrome bo_3: after low intensity reduction, the subunit composition was entirely unaffected. However, after auto-photoreduction under high intensity conditions, the subunits did not enter the separating gel. This is probably due to the formation of photo-cross-linked high molecular mass aggregates of the polypeptides (data not shown).

Photochemical action spectrum

To acquire information on the nature of the chemical species responsible for the electron transfer process, the wavelength dependence of the auto-photoreduction of cytochrome bo_3 was investigated. The auto-photoreduction process was initiated with monochromatic light of a Xe arc lamp in the region of 270–360 nm. The exact number of quanta emitted by the Xe lamp was ascertained by using a chemical actinometer. The photochemical action spectrum exhibits a single broad maximum at 290 nm (Fig. 4, *thick line*). This maximum agrees with an absorbance shoulder at 290 nm in the UV/visible spectrum of the isolated oxidized cytochrome bo_3 (*thin line*). To simulate the absorbance spectrum of the apoprotein, a synthetic mixture of aromatic amino acids present in the same ratios as in the enzyme was prepared. Its absorbance peak centered at 280 nm is different from the maximum found in the protein. A remarkable photochemical potential is retained at wavelength 355 nm and below. To sum up, this electron transfer activity appears to be incompatible with the generic absorbance of aromatic amino acids alone. Thus heme absorbance contributions must also be taken into account to explain the light-driven effect. The relatively long irradiation times necessary to reach full reduction suggest a low quantum yield of the photochemical process.

Optimal conditions for recording FTIR difference spectra

The experimental conditions had to be optimized to obtain reproducible band assignments for the auto-photoreduction spectra. Samples (concentrated cytochrome bo_3 equilibrated in H_2O or D_2O buffer) were prepared, which exhibited a light

TABLE 1 Activity of auto-photoreduced oxidases

	Cytochrome bo_3/e^-/s	Cytochrome aa_3/e^-/s
Control/dark sample	78.0 ± 4.0	1060 ± 58
Photoirradiation (low intensity)	75.0 ± 4.0	1000 ± 44
Photoirradiation (high intensity); CO release	0.4 ± 0.2	9 ± 3

The duroquinol oxidase activity of cytochrome bo_3 of *E. coli* and cytochrome *c* oxidase activity of cytochrome aa_3 from *R. sphaeroides* was measured in the dark and after photoirradiation with light from a defocused (low intensity) and lens-focused Xe lamp (high intensity, CO release conditions), using the ''liquid sample'' handling procedure as described in the Experimental Procedures section. The determined turnover numbers (in electrons per second) are mean values of three measurements taken before and after irradiation for 60 min. Other conditions were as described for the experiment displayed in Fig. 1. Full reduction (and CO release) after photoirradiation was ascertained by static optical and measurement of the CO recombination amplitude at 2 ms after flash photolysis.

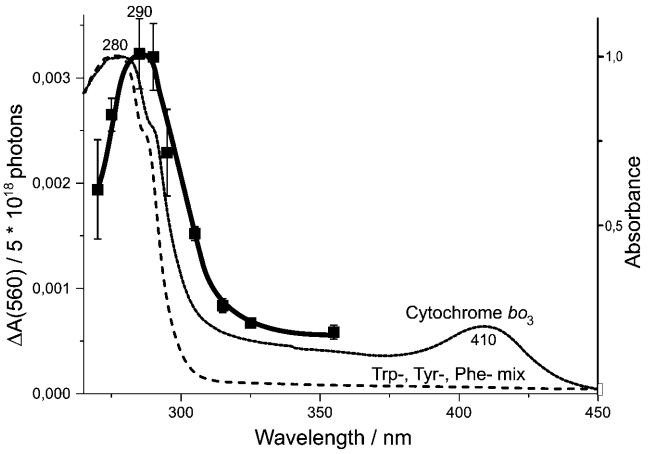

FIGURE 4 Auto-photoreduction of cytochrome bo_3 at different irradiation wavelengths. The absorbance changes per 5×10^{18} photons were calculated from the slopes of the auto-photoreduction spectra obtained after irradiation of single doses (absorbance difference at 560 nm per dose is plotted (*squares, thick line*)). The error bars mark standard deviations of slopes. Absorbance spectra of 1.2 μM cytochrome bo_3 in storage buffer (*continuous line*) and of model compounds (mix of aromatic amino acids in the same stoichiometric ratios as in cytochrome bo_3 (CyoABCD has 80 tryptophanes, 72 tyrosines, and 201 phenylalanines (*dashed line*)). Both spectra were normalized with respect to the absorbances at 280 nm.

transmission of 4–6.5% of maximum intensity, while taking into account the highest absorbances produced by the amide I and water bending modes. The maximum permitted absorbances of 0.002 were thus obtained at a 1662/1657 cm^{-1} difference band (see below). Application of smaller sample amounts leads to insufficient difference signal amplitudes. On the other hand, much higher sample amounts gave reasonable absorbances, but due to the low transmittance in the amide I region the noise level was increased significantly. Absorbance band distortions have to be taken into account, and spectral alterations, owing to phase errors implicated with the Fourier transformation, also have to be considered. The amide I band could be optimally evaluated by comparative analysis (e.g., by double difference spectra) in samples exhibiting ~10% transmission. Having adjusted this condition (i.e., relatively low sample amounts), due to low signal intensities, it is difficult to evaluate slight absorbance variations outside the amide I spectral region.

General effect of photoirradiation on FTIR spectra (cytochrome bo_3)

In the past, several people, including ourselves, have used FMN/EDTA as a caged electron donor for various heme-copper oxidases (Lübben and Gerwert, 1996; Lübben et al., 1999; Yamazaki et al., 1999a) in infrared spectroscopy. The goal of this study is to produce redox FTIR spectra from cytochrome oxidases in the absence of (externally added) artificial electron donors to avoid spectral disturbance from byproducts of the electron transfer reaction. Therefore, redox spectra generated by different techniques were compared. Fig. 5 *A* displays the redox FTIR spectra of cytochrome bo_3 recorded in the range of 1690–1990 cm^{-1}, using different light sources and reaction conditions. At ~1960 cm^{-1}, the adducts of CO with ferrous high-spin heme (Fiamingo et al., 1986; Hill et al., 1992; Shapleigh et al., 1992; Lemon et al., 1993; Einarsdottir et al., 1993; Rich and Breton, 2001) could be observed. CO release occurs under intense irradiation seen in the laser-induced spectrum (Fig. 5 *A*, *top*). The use of lower light intensities from a Xe lamp with and without the presence of FMN (Fig. 5 *A*, *middle* and *bottom*) yields no or insignificant release of CO. The light-induced evolution of difference spectra by photoreduction and auto-photoreduction is compared on an expanded scale in Fig. 5 *B*. The similarity of spectra generated by both methods above 1680 cm^{-1} is evident. In the photoreduction spectra, the so-called fingerprint region of the spectrum is partially obscured by the reaction products from the chemical electron transfer reaction. In the photoreduction spectra alone, the simple subtraction of absorbance contributions by caged compounds is not possible, because the oxidation of EDTA takes place only in the presence of a suitable electron acceptor, specifically the oxidase itself. In contrast, the auto-photoreduction spectra are remarkably reproducible; they are free of signals from photolytic byproducts (Fig. 5), e.g., the decomposition of EDTA, so in principle the spectra could be used for correction of contributions from caged compounds. Peaks at ~1500 cm^{-1} and 1320 cm^{-1} in the auto-photoreduced spectrum are above the noise, and, in the absence of spectral contributions from caged compounds, can now be attributed to the protein itself. Notably, the majority of absorbance bands can be resolved in both types of photo-induced FTIR difference spectra. The spectral region of 1680–1800 cm^{-1} is especially informative for the analysis of protonated carboxyl groups. All three ways of inducing the redox transition discussed above result in similar patterns at 1744/1735 cm^{-1} (Fig. 5 *A*), reflecting a redox-driven environmental change, which had been previously assigned to ν(C=O) signals from glutamic acid-286 (Lübben et al., 1999; Hellwig et al., 1998) located in the center of the D-channel of the catalytic subunit I. The band positions of absorbance maxima and minima from photoreduction were almost identical with those recorded by means of electrochemical equilibration (Hellwig et al., 1999a). These difference absorbance features were much less pronounced in mutants containing aspartic acid in place of glutamic acid-286 (Lübben et al., 1999). The different absorbance intensities of glutamic and of aspartic acid had been related to dissimilar interactions of the carboxyl groups with the hydrogen-bonded network located in the proton channel (Puustinen et al., 1997). At 1198 cm^{-1}, there is a fingerprint absorbance feature, which is probably related to the ν(C-O) of glutamic acid (Barth, 2000) and which apparently arises from the same environmental change that was described for the ν(C=O) band. This small band disappears

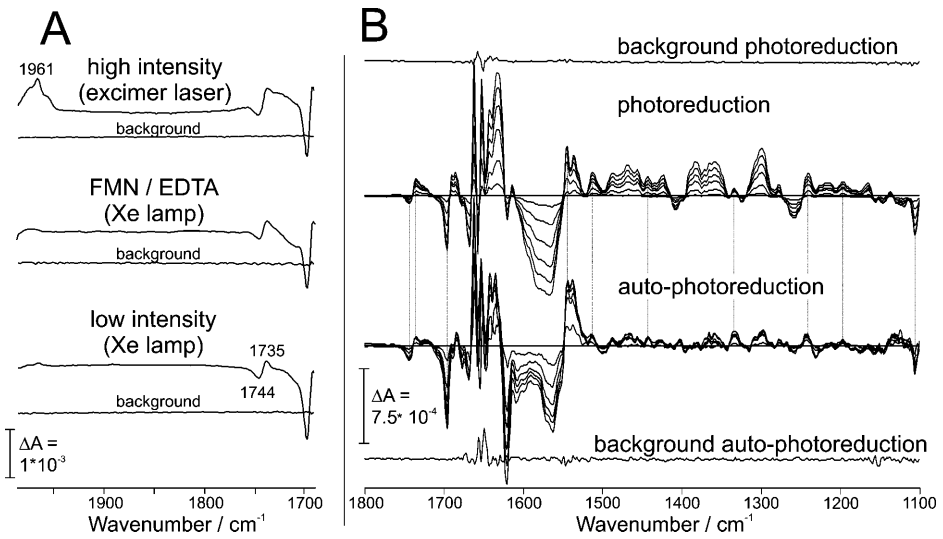

FIGURE 5 FTIR redox difference spectra (reduced-oxidized) of cytochrome bo_3 using various electron donors. The background spectra provide information on the noise level and the sample stability. They correspond to the ''difference spectra'' that are obtained, if no photoreaction takes place; 400 scans in the dark were averaged (equivalent to the ''reference spectrum''), then another 400 scans were averaged immediately thereafter (equivalent to the ''sample spectrum'' without photoirradiation). The differences between both spectra were calculated and assigned as ''background'' spectra in Figs. 5, 6, and 7. In the entire spectral range, the background ''spectra'' ideally represent zero lines parallel to the abscissa; they are colinear with the flat region (from 1750 cm^{-1} to >1800 cm^{-1}) of the photoinduced difference spectra in Figs. 5, 6, and 7, and they can be easily extrapolated to the other displayed spectral regions. For better visibility, the background lines are offset from the photoinduced spectra. The upward deflecting (positive) bands pertain to the photoreduced and the downward deflecting (negative) bands to the oxidized states of the protein. (*A*) Top: auto-photoreduction induced with monochromatic high-intensity excimer laser with irradiation wavelength of 308 nm after 2500 pulses with 100 mJ. Center: sample reduced by caged electron donor FMN/EDTA by Xe lamp (25 min). Bottom: auto-photoreduction with nonfocused Xe lamp; total irradiation time was 25 min. (*B*) Comparison of photoreduction in the presence of FMN/EDTA (halogen lamp, 75 μg sample amount) and of auto-photoreduction (Xe lamp, low intensity, 37 μg sample amount) on the FTIR difference spectra of cytochrome bo_3. Measurements were performed as described in the Experimental Procedures section; only the spectra recorded after 40, 100, 160, 220, 280, 340, and 400 s (halogen lamp) and after 320, 800, 1280, 1760, 2240, 2720, and 3200 s (Xe lamp) of irradiation are displayed. The spectra recorded at higher sample amounts by photo-reduction exhibit an apparently higher signal/noise ratio due to spectral downscaling to 0.75×10^{-3} at 1696–1691 cm^{-1}, a value that is regularly obtained by auto-photoreduction.

upon solvent exchange to D_2O (not shown) and it is absent in mutants affecting Glu-286 (e.g., in Glu-286-Asp (Fig. 6) or Glu-286-Gln (not shown)), but it is found reproducibly in other mutant oxidases in which Glu-286 is preserved (Fig. 6).

Auto-photoreduction FTIR spectra of cytochrome aa_3

The conditions optimized in the experiments described were applied to cytochrome *c* oxidases of bacteria and mitochondria to probe the universality of mild auto-photoreduction; the obtained redox FTIR difference spectra are shown in Fig. 7. The carbonyl region (Fig. 7, *inserts*) enables the identification of the previously detected typical band signature at 1745/1737 cm^{-1} (*R. sphaeroides*) (Lübben and Gerwert, 1996) or at 1749/1743 cm^{-1} (mitochondrial) (Hellwig et al., 1999b), assigned to the homolog of the *E. coli* Glu-286, as discussed above. In both cytochrome *c* oxidases, redox-dependent changes in the amide I region of ~1620–1650 cm^{-1} are evident (Fig. 7), which is a further verification of molecular stability after photoirradiation. The data are highly reproducible, which is especially important for the fingerprint region; the FTIR difference spectra confirm our previous notion that spectral perturbations found with the reductant FMN/EDTA are also absent in this class of heme-copper oxidases. Although both cytochrome *c* oxidases are functionally equivalent, their redox FTIR spectra are remarkably different, when regions between 1700 and 1750 cm^{-1} are compared. For example, the carbonyl signature band at 1745/1737 cm^{-1} of the *R. sphaeroides* oxidase is moved to higher wavenumbers in the mitochondrial enzyme, whereas the positive absorbance change of the latter is shifted to 1717 cm^{-1}. This could be due to the extra subunits in the mitochondrial oxidase, which provide the enzyme with a number of additional functional groups that may be involved within the redox-induced rearrangement. Clear band shifts are seen in the difference spectra after solvent replacement by D_2O, which result from oscillator mass enhancements after proton/deuteron exchange. The fingerprint region is resolved unambiguously; the spectral comparison of *Rhodobacter* oxidase mutants dissolved in H_2O and D_2O will elucidate a number of specific band assignments in the respective region.

DISCUSSION

The phenomenon of auto-photoreduction is known for a number of heme proteins (Pierre et al., 1982; Bazin et al., 1982; Gu et al., 1993; Sakai et al., 2000). Recently, the formation of the peroxy and oxoferryl complexes was shown to be induced by irradiation of cytochrome *c* oxidase with light <300 nm in the presence of oxygen (Brooks et al., 1997). In the study presented here we have demonstrated that

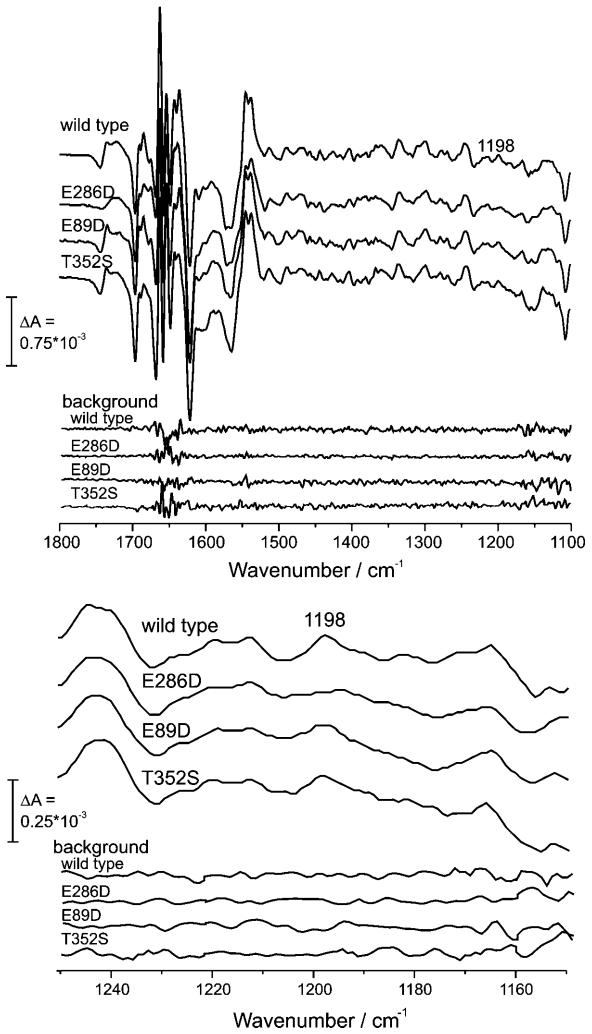

FIGURE 6 FTIR redox difference spectra (reduced-oxidized, auto-photoreduction) of wild-type and of various mutants of cytochrome bo_3. Top, overview spectra; bottom, extension of the fingerprint region around 1200 cm^{-1}.

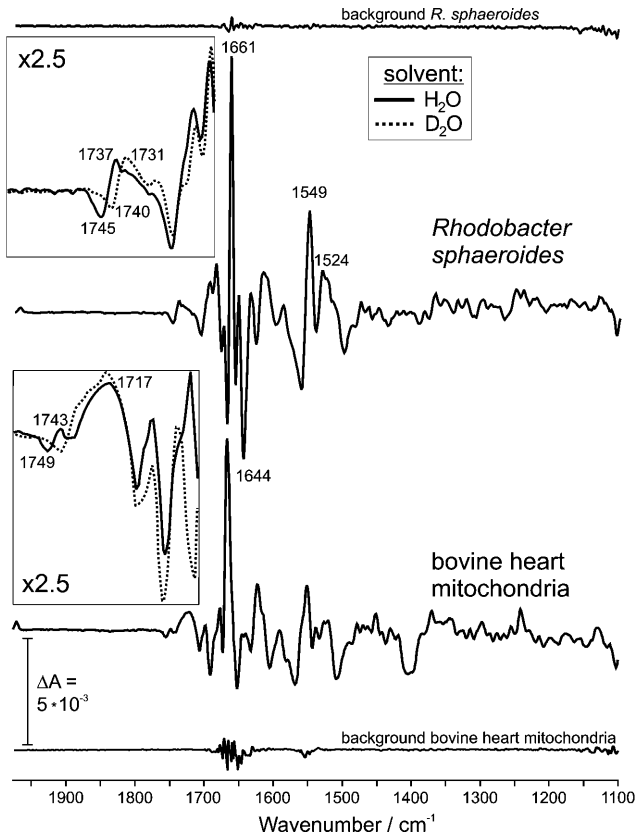

FIGURE 7 FTIR spectra (reduced-oxidized, auto-photoreduction) of cytochrome *c* oxidases of *R. sphaeroides* (*top*) and of bovine heart mitochondria (*bottom*) with Xe lamp at low-light intensity. (*Insets*) Closeup of the carbonyl region of samples, dissolved in H_2O and D_2O.

different heme-coppper oxidases reach their fully reduced state when internal electron transfer is driven anaerobically by ultraviolet light. These oxidases undergo noninvasive auto-photoreduction if reaction conditions avoiding release of carbon monoxide are maintained.

Release of carbon monoxide

Auto-photoreduction could be measured at low light intensities; significant release of CO was observed at a much higher radiation. The mechanism of CO production is of particular interest and will be discussed in greater detail elsewhere. In the context of our objectives, i.e., to establish appropriate auto-photoreduction conditions, CO release has to be suppressed to ensure that the protein is in a chemically unperturbed state. The heme *a* and *o* groups (i.e., the high-spin hemes) are most probably the source of carbon monoxide, because no other photochemically active additives were present. In the case of cytochrome bo_3, the heme *o* group is preferentially decomposed during high-intensity irradiation, whereas the low-spin heme *b* group remains unaffected (Fig. 3). One might conclude that farnesylated heme groups are more susceptible to light-induced decomposition than the short-chain substituted iron-protoporphyrin. For the practical setup of noninvasive reaction conditions, we used the liberation of CO as an indicator of irradiation intensities that could photochemically disrupt the oxidase.

Nature of the reduced state

The photoreductive irradiation was usually stopped at ~90–100% of heme reduction, as it was obtained in parallel samples and quantified by FMN/EDTA as an electron donor. Three (ubiquinol oxidase) or four (cytochrome *c* oxidase) electrons should fill up the redox sites in their thermodynamically defined order, i.e., the centers Cu_B, high-spin heme, low-spin heme, and Cu_A. The degree of reduction was measured by the absorbance of the heme α-band, which is, strictly speaking, indicative of the low-potential redox

centers. Thus, at 90% auto-photoreduction, the ubiquinol oxidase (which has no Cu_A) is three-electron reduced. In cytochrome *c* oxidase, the photoreduced state of the Cu_A center cannot be proven by our experiments (the reaction was not monitored at 830 nm), but due to electron equilibration the enzyme should be converted to the four-electron-reduced form. By assuming values of the midpoint potentials for the Cu_A and heme α centers of +240 mV and +230 mV (Wikström et al., 1981), 93% of the Cu_A sites are reduced at a heme reduction level of 90%. Einarsdottir and co-workers have created the oxoferryl state of cytochrome *c* oxidase by auto-photoreduction in the presence of oxygen (Brooks et al., 1997). In contrast, our experiments are carried out anaerobically with the enzyme ending up in the fully reduced state.

Which chemical groups could be involved in the photoreaction?

The elucidation of the mechanism of photoinduced electron transfer in cytochrome oxidases far exceeds the scope of this report. A number of different effects may interact mutually.

Isolated porphyrins can act as photosensitizers in various reactions (Reddi et al., 1987); if bound to heme apoproteins the cofactors have been shown to be involved in auto-photoreduction (Gu et al., 1993; Sakai et al., 2000). Photochemical action spectra show a single maximum of 290 nm, which clearly differs from the absorbance at 280 nm of aromatic amino acid side chains. However, this peak maximum of 290 nm cannot unequivocally be assigned to heme absorbance. The light-induced electron transfer may be explained by a complex mechanism, which could be composed of different (cooperating) photochemical events.

We conclude that at least the primary activation process in photo-induced electron transfer is due to the action of heme groups, which leads to a Fe^{2+}/porphyryl radical intermediate state (Sakai et al., 2000). Due to the high oxidation power of the porphyryl radical generated upon photon absorption, estimated to be from +1.2 to +1.4 V (versus normal hydrogen electrode) (Furhop et al., 1973; Kadish and Morrison, 1976), it should readily accept electrons from components that have lower redox potential; i.e., the aromatic amino acids tyrosine and tryptophan have to be taken into account, because their midpoint redox potentials are $E_0 = +0.94$ and +1.05 V (measured in free solution) (DeFelippis et al., 1989). It should be noted that the spectra of tyrosinate (Edelhoch, 1967) and of transiently photo-activated tyrosine (Bent and Hayon, 1975) (triplet state ^{3}Tyr) exhibit absorbance maxima at ~290 nm, which corresponds to the peak in our observed photochemical action spectra of cytochrome bo_3 oxidase.

The external additives, tris and the detergent decylmaltoside, are excluded from the oxidase reaction center, because the heme groups of the protein are deeply embedded in the membrane and are thus nonaccessible to these small molecules, which are freely dissolved in the aqueous phase. A similar explanation holds for the ineffectiveness of externally added tryptophan to stimulate photoreduction of the cytochrome oxidase. In contrast, addition of this amino acid facilitates reduction of certain heme proteins that have their cofactors more strongly exposed to the solvent (Pierre et al., 1982; Sakai et al., 2000). It is deduced that the final electron donor for heme groups arises from the protein interior.

Alternatively, hydroxy or water ligands to the high-spin heme and Cu_B (Wikström et al., 2000) may be considered to act as reductants due to their proximity to the internal photoactivated radical groups. It is also probable that the electrons are abstracted from water molecules located in the aqueous internal spaces of the protein. Both the D- and K-proton channels contain bound water (Ostermeier et al., 1997), which could involve different protein groups/contact sites.

Redox investigation by FTIR spectroscopy

The primary purpose of this study was to probe auto-photoreduction and to record infrared spectra of the fingerprint region. This is a prerequisite for detailed band assignment in the difference spectra and for identification of molecular groups involved in the intramolecular electron transfer, and thus important for understanding the reaction mechanism of the protein. The auto-photoreduction reaction works equally with different heme-copper oxidases of the ubiquinol and cytochrome *c* subclasses. The MIR spectra have superior quality, because no disruptive spectral contributions from the caged reaction with FMN/EDTA were present after auto-photoreduction. The photolytic conditions can be controlled closely by the FTIR method, because the CO binding to the high-spin heme can be easily monitored. It is possible to identify extremely weak bands in the fingerprint region with this technique, e.g., the absorbance band at 1198 cm^{-1} in cytochrome bo_3. An even higher signal/noise ratio may be achieved by further increase of the sample concentration, as long as no quantitative comparisons of the strongly absorbing amide I band are required (see below).

General usability of this novel redox FTIR spectroscopic technique

Anaerobic auto-photoreduction is a phenomenon observed with heme-copper oxidases, which most probably represents a composite of different potential light-driven reactions. At present, these are difficult to explain in detail. Whatever the exact photochemical mechanisms are, it is important to note that the photochemical reaction conditions can be carefully adjusted to avoid disruptive effects on the protein and preserve its structural and functional integrity. Auto-photoreduction is a valuable tool for studying various different heme-copper cytochrome oxidases at the molecular

level with FTIR. It allows the observation of absorbance changes of functional protein groups in different spectral ranges. For the purpose of FTIR spectroscopy, band assignments are carried out by comparison of difference spectra generated from wild-type oxidase with those of site-directed mutants or isotopically labeled variants. In any case, molecular events contributing to the photoreaction, which are not observed on the aforementioned structural/functional level, may not leave their imprints in the measured spectra, simply because those would be canceled out by calculation of the double difference spectra.

The described technique allows the light-induced redox spectra to be recorded without the undesirable absorbance contributions from externally added caged compounds, thus facilitating the analysis of absorbance peaks in a wider spectral region. It should be emphasized that this method is very reliable; it can be operated at much lower experimental and financial expenses than the rather intricate electrochemical equilibration techniques. If the sample concentrations were adjusted to result in at least 4% transmission in the observed spectral range, the auto-photoreduction FTIR spectra would be very reproducible and exhibit a high signal/noise ratio, especially in the infrared fingerprint region. This will also help us to resolve in future bands that had low intensity or which were invisible in previous experiments.

In addition to heme-copper oxidases, we have used this method to observe FTIR spectra with the respiratory complex III (the so-called bc_1 complex) of bacteria, cytochrome *c*, met-myoglobin, and met-hemoglobin (to be published elsewhere). Auto-photoreduction therefore seems to be a tool that can be universally applied to study reaction mechanisms of heme proteins at atomic level.

We thank the reviewers for helpful suggestions. We are especially grateful to Prof. Klaus Gerwert, who supported us by maintenance of the FTIR spectroscopic infrastructure.

This work was supported by the Volkswagen-Stiftung and the Fonds der Chemischen Industrie.

REFERENCES

Adar, F., and M. Erecinska. 1979. Photoreductive titration of the resonance Raman spectra of cytochrome oxidase in whole mitochondria. *Biochemistry.* 18:1825–1829.

Adar, F., and T. Yonetani. 1978. Resonance Raman spectra of cytochrome oxidase. Evidence for photoreduction by laser photons in resonance with the Soret band. *Biochim. Biophys. Acta.* 502:80–86.

Babcock, G. T., and I. Salmeen. 1979. Resonance Raman spectra and optical properties of oxidized cytochrome oxidase. *Biochemistry.* 18: 2493–2498.

Babcock, G. T., and M. Wikström. 1992. Oxygen activation and the conservation of energy in cell respiration. *Nature.* 356:301–309.

Barth, A. 2000. The infrared absorption of amino acid side chains. *Prog. Biophys. Mol. Biol.* 74:141–173.

Bartocci, C., F. Scandola, A. Ferri, and V. Carassiti. 1980. Photoreduction of hemin in alcohol-containing mixed solvents. *J. Am. Chem. Soc.* 102:7067–7072.

Bazin, M., J. Pierre, P. Debey, and R. Santus. 1982. One-electron photoreduction of bacterial cytochrome P-450 by ultraviolet light. II. A study using laser flash photolysis of the dynamics of the reduction of bacterial cytochrome P-450 in the presence of carbon monoxide. The role of the protein conformation. *Eur. J. Biochem.* 124:539–544.

Bent, D. V., and E. Hayon. 1975. Excited state chemistry of aromatic amino acids and related peptides. I. Tyrosine. *J. Am. Chem. Soc.* 97:2599–2606.

Brooks, J. L., A. Sucheta, and Ö. Einarsdottir. 1997. Light-induced spectral changes in fully oxidized cytochrome *c* oxidase in the presence of oxygen. *Biochemistry.* 36:6336–6342.

DeFelippis, M. R., C. P. Murthy, M. Faraggi, and M. H. Klapper. 1989. Pulse radiolytic measurement of redox potentials: the tyrosine and tryptophan radicals. *Biochemistry.* 28:4847–4853.

Edelhoch, H. 1967. Spectroscopic determination of tryptophan and tyrosine in proteins. *Biochemistry.* 6:1948–1954.

Einarsdottir, Ö., R. B. Dyer, D. D. Lemon, P. M. Killough, S. M. Hubig, S. J. Atherton, J. J. Lopez-Garriga, G. Palmer, and W. H. Woodruff. 1993. Photodissociation and recombination of carbonmonoxy cytochrome oxidase: dynamics from picoseconds to kiloseconds. *Biochemistry.* 32: 12013–12024.

Ferguson-Miller, S., and G. T. Babcock. 1996. Heme/copper terminal oxidases. *Chem. Rev.* 96:2889–2907.

Fiamingo, F. G., R. A. Altschuld, and J. O. Alben. 1986. Alpha and beta forms of cytochrome *c* oxidase observed in rat heart myocytes by low temperature Fourier transform infrared spectroscopy. *J. Biol. Chem.* 261:12976–12987.

Furhop, J.-H., K. M. Kadish, and D. G. Davis. 1973. The redox behavior of metallo octaethylporphyrins. *J. Am. Chem. Soc.* 95:5140–5147.

Garcia-Horsman, J. A., B. Barquera, J. Rumbley, J. Ma, and R. B. Gennis. 1994. The superfamily of heme-copper respiratory oxidases. *J. Bacteriol.* 176:5587–5600.

Gu, Y., P. Li, T. Sage, and P. M. Champion. 1993. Photoreduction of heme proteins: spectroscopic studies and cross-section measurements. *J. Am. Chem. Soc.* 115:4993–5004.

Heller, H. G., and J. R. Langan. 1981. Photochromic heterocyclic fulgides. Part 3. The use of (E)-a-(2,5-dimethyl-3-furylethylidene)(isopropylidene) succinic anhydride as a simple convenient chemical actinometer. *J. Chem. Soc. Perkin.* II:341–343.

Hellwig, P., J. Behr, C. Ostermeier, O. M. Richter, U. Pfitzner, A. Odenwald, B. Ludwig, H. Michel, and W. Mäntele. 1998. Involvement of glutamic acid 278 in the redox reaction of the cytochrome *c* oxidase from *Paracoccus denitrificans* investigated by FTIR spectroscopy. *Biochemistry.* 37:7390–7399.

Hellwig, P., T. Mogi, F. L. Tomson, R. B. Gennis, J. Iwata, H. Miyoshi, and W. Mäntele. 1999a. Vibrational modes of ubiquinone in cytochrome bo_3 from *Escherichia coli* identified by Fourier transform infrared difference spectroscopy and specific ^{13}C labeling. *Biochemistry.* 38: 14683–14689.

Hellwig, P., B. Rost, U. Kaiser, C. Ostermeier, H. Michel, and W. Mäntele. 1996. Carboxyl group protonation upon reduction of the *Paracoccus denitrificans* cytochrome *c* oxidase: direct evidence by FTIR spectroscopy. *FEBS Lett.* 385:53–57.

Hellwig, P., T. Soulimane, G. Buse, and W. Mantele. 1999b. Similarities and dissimilarities in the structure-function relation between the cytochrome c oxidase from bovine heart and from Paracoccus denitrificans as revealed by FT-IR difference spectroscopy. *FEBS Lett.* 458:83–86.

Hill, J., V. C. Goswitz, M. Calhoun, J. A. Garcia-Horsman, L. Lemieux, J. O. Alben, and R. B. Gennis. 1992. Demonstration by FTIR that the *bo*-type ubiquinol oxidase of *Escherichia coli* contains a heme-copper binuclear center similar to that in cytochrome *c* oxidase and that proper assembly of the binuclear center requires the *cyoE* gene product. *Biochemistry.* 31:11435–11440.

Iwaki, M., J. Breton, and P. R. Rich. 2002. ATR-FTIR difference spectroscopy of the P(M) intermediate of bovine cytochrome *c* oxidase. *Biochim. Biophys. Acta.* 1555:116–121.

Iwata, S., C. Ostermeier, B. Ludwig, and H. Michel. 1995. Structure at 2.8 Å resolution of cytochrome *c* oxidase from *Paracoccus denitrificans*. *Nature*. 376:660–669.

Kadish, K. M., and M. M. Morrison. 1976. Solvent and substituent effects on the redox reactions of para-substituted tetraphenylporphyrin. *J. Am. Chem. Soc*. 98:3326–3328.

Kita, K., K. Konishi, and Y. Anraku. 1984. Terminal oxidases of *Escherichia coli* aerobic respiratory chain. I. Purification and properties of cytochrome b_{562}-*o* complex from cells in the early exponential phase of aerobic growth. *J. Biol. Chem.* 259:3368–3374.

Laemmli, U. K. 1970. Cleavage of structural proteins during the assembly of the head of bacteriophage T4. *Nature*. 227:680–685.

Lemon, D. D., M. W. Calhoun, R. B. Gennis, and W. H. Woodruff. 1993. The gateway to the active site of heme-copper oxidases. *Biochemistry*. 32:11953–11956.

Lübben, M., and K. Gerwert. 1996. Redox FTIR difference spectroscopy using caged electrons reveals contributions of carboxyl groups to the catalytic mechanism of haem-copper oxidases. *FEBS Lett*. 397:303–307.

Lübben, M., and K. Morand. 1994. Novel prenylated hemes as cofactors of cytochrome oxidases. Archaea have modified hemes A and O. *J. Biol. Chem*. 269:21473–21479.

Lübben, M., A. Prutsch, B. Mamat, and K. Gerwert. 1999. Electron transfer induces side-chain conformational changes of glutamate-286 from cytochrome bo_3. *Biochemistry*. 38:2048–2056.

Nyquist, R. M., D. Heitbrink, C. Bolwien, R. B. Gennis, and J. Heberle. 2003. Direct observation of protonation reactions during the catalytic cycle of cytochrome *c* oxidase. *Proc. Natl. Acad. Sci. USA*. 100:8715–8720.

Nyquist, R. M., D. Heitbrink, C. Bolwien, T. A. Wells, R. B. Gennis, and J. Heberle. 2001. Perfusion-induced redox differences in cytochrome c oxidase: ATR/FT-IR spectroscopy. *FEBS Lett*. 505:63–67.

Ogura, T., S. Yoshikawa, and T. Kitagawa. 1985. Resonance Raman study on photoreduction of cytochrome *c* oxidase: distinction of cytochromes *a* and a_3 in the intermediate oxidation states. *Biochemistry*. 24:7746–7752.

Ostermeier, C., A. Harrenga, U. Ermler, and H. Michel. 1997. Structure at 2.7 Å resolution of the *Paracoccus denitrificans* two-subunit cytochrome *c* oxidase complexed with an antibody F_v fragment. *Proc. Natl. Acad. Sci. USA*. 94:10547–10553.

Pereira, M. M., M. Santana, and M. Teixeira. 2001. A novel scenario for the evolution of haem-copper oxygen reductases. *Biochim. Biophys. Acta*. 1505:185–208.

Pierre, J., M. Bazin, P. Debey, and R. Santus. 1982. One-electron photoreduction of bacterial cytochrome P-450 by ultraviolet light. I. Steady-state irradiations. *Eur. J. Biochem*. 124:533–537.

Prutsch, A., C. Lohaus, B. Green, H. E. Meyer, and M. Lübben. 2000. Multiple posttranslational modifications at distinct sites contribute to heterogeneity of the lipoprotein cytochrome bo_3. *Biochemistry*. 39:6554–6563.

Puustinen, A., J. A. Bailey, R. B. Dyer, S. L. Mecklenburg, M. Wikström, and W. H. Woodruff. 1997. Fourier transform infrared evidence for connectivity between Cu_B and glutamic acid 286 in cytochrome bo_3 from *Escherichia coli*. *Biochemistry*. 36:13195–13200.

Puustinen, A., J. E. Morgan, M. Verkhovsky, J. W. Thomas, R. B. Gennis, and M. Wikström. 1992. The low-spin heme site of cytochrome *o* from *Escherichia coli* is promiscuous with respect to heme type. *Biochemistry*. 31:10363–10369.

Puustinen, A., and M. Wikström. 1991. The heme groups of cytochrome *o* from *Escherichia coli*. *Proc. Natl. Acad. Sci. USA*. 88:6122–6126.

Reddi, E., C. R. Lambert, G. Jori, and M. A. Rodgers. 1987. Photokinetic and photophysical measurements of the sensitized photooxidation of the tryptophyl residue in N-acetyl tryptophanamide and in human serum albumin. *Photochem. Photobiol*. 45:345–351.

Rich, P. R., and J. Breton. 2001. FTIR studies of the CO and cyanide adducts of fully reduced bovine cytochrome *c* oxidase. *Biochemistry*. 40:6441–6449.

Rich, P. R., and J. Breton. 2002. Attenuated total reflection Fourier transform infrared studies of redox changes in bovine cytochrome c oxidase: resolution of the redox Fourier transform infrared difference spectrum of heme a_3. *Biochemistry*. 41:967–973.

Rumbley, J. N., E. Furlong Nickels, and R. B. Gennis. 1997. One-step purification of histidine-tagged cytochrome bo_3 from *Escherichia coli* and demonstration that associated quinone is not required for the structural integrity of the oxidase. *Biochim. Biophys. Acta*. 1340: 131–142.

Sakai, H., H. Onuma, M. Umeyama, S. Takeoka, and E. Tsuchida. 2000. Photoreduction of methemoglobin by irradiation in the near-ultraviolet region. *Biochemistry*. 39:14595–14602.

Salmeen, I., L. Rimai, and G. Babcock. 1978. Raman spectra of heme *a*, cytochrome oxidase-ligand complexes, and alkaline denatured oxidase. *Biochemistry*. 17:800–806.

Saraste, M. 1990. Structural features of cytochrome oxidase. *Q. Rev. Biophys*. 23:331–366.

Saraste, M., L. Holm, L. Lemieux, M. Lübben, and J. van der Oost. 1991. The happy family of cytochrome oxidases. *Biochem. Soc. Trans*. 19: 608–612.

Shapleigh, J. P., J. J. Hill, J. O. Alben, and R. B. Gennis. 1992. Spectroscopic and genetic evidence for two heme-Cu-containing oxidases in *Rhodobacter sphaeroides*. *J. Bacteriol*. 174:2338–2343.

Smith, P. K., R. I. Krohn, G. T. Hermanson, A. K. Mallia, F. H. Gartner, M. D. Provenzano, E. K. Fujimoto, N. M. Goeke, B. J. Olson, and D. C. Klenk. 1985. Measurement of protein using bicinchoninic acid. *Anal. Biochem*. 150:76–85.

Trumpower, B. L., and R. B. Gennis. 1994. Energy transduction by cytochrome complexes in mitochondrial and bacterial respiration: the enzymology of coupling electron transfer reactions to transmembrane proton translocation. *Annu. Rev. Biochem*. 63:675–716.

Tsukihara, T., H. Aoyama, E. Yamashita, T. Tomizaki, H. Yamaguchi, K. Shinzawa-Itoh, R. Nakashima, R. Yaono, and S. Yoshikawa. 1996. The whole structure of the 13-subunit oxidized cytochrome *c* oxidase at 2.8 Å. *Science*. 272:1136–1144.

Vanneste, W. H. 1966. The stoichiometry and absorption spectra of components *a* and *a*-3 in cytochrome *c* oxidase. *Biochemistry*. 5:838–848.

Wikström, M., A. Jasaitis, C. Backgren, A. Puustinen, and M. I. Verkhovsky. 2000. The role of the D- and K-pathways of proton transfer in the function of the haem-copper oxidases. *Biochim. Biophys. Acta*. 1459:514–520.

Wikström, M., K. Krab, and M. Saraste. 1981. Cytochrome Oxidase: A Synthesis. Academic Press, New York.

Yamazaki, Y., H. Kandori, and T. Mogi. 1999a. Effects of subunit I mutations on redox-linked conformational changes of the *Escherichia coli bo*-type ubiquinol oxidase revealed by Fourier-transform infrared spectroscopy. *J. Biochem. (Tokyo)*. 126:194–199.

Yamazaki, Y., H. Kandori, and T. Mogi. 1999b. Fourier-transform infrared studies on conformation changes in *bd*-type ubiquinol oxidase from *Escherichia coli* upon photoreduction of the redox metal centers. *J. Biochem. (Tokyo)*. 125:1131–1136.

Zhen, Y., J. Qian, K. Follmann, T. Hayward, T. Nilsson, M. Dahn, Y. Hilmi, A. G. Hamer, J. P. Hosler, and S. Ferguson-Miller. 1998. Overexpression and purification of cytochrome *c* oxidase from *Rhodobacter sphaeroides*. *Protein Expr. Purif*. 13:326–336.